PERGAMON

Energy Conversion and Management 44 (2003) 1755–1772

ENERGY CONVERSION & MANAGEMENT

www.elsevier.com/locate/enconman

Efficient segmented thermoelectric unicouples for space power applications

Mohamed S. El-Genk [a,*], Hamed H. Saber [a], Thierry Caillat [b]

[a] *Department of Chemical and Nuclear Engineering, Institute for Space and Nuclear Power Studies, The University of New Mexico, Albuquerque, NM 87131, USA*

[b] *Jet Propulsion Laboratory, Californian Institute of Technology, 4800 Oak Grove Drive, MS 277-207, Pasadena, CA 91109, USA*

Received 13 May 2002; accepted 2 September 2002

Abstract

This paper compares the performance of SiGe ($Si_{0.8}Ge_{0.2}$) and skutterudite segmented thermoelectric unicouples (STUs) at a hot side temperature of 973 K and cold side temperatures of 300, 573 and 673 K and for the same total length and cross sectional dimensions of the p-leg. The area of the n-leg and lengths of and the interfacial temperatures between segments of various materials in the STU legs are determined using a global optimization methodology. Results indicate that the STUs could potentially achieve peak efficiencies of 7.8% and 14.7% when operated at a cold side temperature of 573 K, typical of that in current radioisotope thermoelectric generators (RTGs), and 300 K, respectively. These efficiencies are 55% and 99% higher, respectively, than for SiGe at the same temperatures. However, due to the higher density of skutterudite, the electrical power densities corresponding to the peak efficiencies of the STUs are 39 and 109 W_e/kg versus 92 and 232 W_e/kg for SiGe at cold side temperatures of 573 K and 300 K, respectively. On the other hand, the heat inputs and heat rejection powers for the STUs are 42–55% and 39–53%, respectively, of those for SiGe at the peak efficiency and 70–75% and 67–77% of those of SiGe, respectively, at the peak electric power density. Therefore, when used in RTGs, STUs could halve the $^{238}PuO_2$ fuel mass and the radiator area, while operating at >45% higher electrical power density (>7 W_e/kg) than SiGe in current RTGs (~5.5 W_e/kg).

Keywords: Segmented thermoelectric; Skutterudites; Energy conversion; Space exploration; Radioisotope power systems; Radioisotope thermoelectric generators (RTGs); Space nuclear reactor power systems

* Corresponding author. Tel.: +1-505-277-5442; fax: +1-505-277-2814.
E-mail address: mgenk@unm.edu (M.S. El-Genk).

0196-8904/02/$ - see front matter
PII: S0196-8904(02)00217-0

Nomenclature

A	cross section area (m^2)
ℓ	segment length (m)
I	electric current (A)
L	total length of STU
P_e	electrical power (W)
T	temperature (K)
V_L	load voltage (V)
ZT	dimensionless figure-of-merit

Greek symbols

η	conversion efficiency (%)
ΔT	temperature difference across segment (K)

Subscripts

c	cold side
h	hot side
n	n-leg
p	p-leg

1. Introduction

Thermoelectric unicouples made of silicon germanium alloys ($Si_{0.8}Ge_{0.2}$ and $Si_{0.63}Ge_{0.38}$) have been used during the last four decades in more than 35 radioisotope thermoelectric generators (RTGs; Fig. 1) to convert the thermal power generated by a radioisotope heat source to electricity for numerous planetary exploration missions. These unicouples operate typically at hot and cold side temperatures of 1175–1273 and 573 K, respectively [2,15]. SiGe/GaP thermoelectric modules have been used in the United States SP-100 nuclear reactor space power system, generating >100 kW_e for more than 10 years (Fig. 2). These thermoelectric modules operate at hot and cold side temperatures of ~1350 and 820 K, respectively, for an overall system efficiency of 4.4% and electrical power density of ~23.5 W_e/kg (or specific mass of 42.6 kg/kW_e). For a lower heat source temperature (<800 K), thermoelectric devices made of lead telluride alloys have been used in the only space nuclear reactor power system ever launched by the United States, SNAP-10A [1].

In RTGs (Fig. 1), SiGe unicouples partially convert the heat generated by the radioactive decay of ^{238}Pu in $^{238}PuO_2$ fuel pellets, encapsulated in the general purpose heat source (GPHS) modules [10,15]. Each GPHS module encapsulates four $^{238}PuO_2$ fuel pellets and produces about 250 W_{th} for fresh fuel at the beginning-of-mission. Because the half life of ^{238}Pu is 86.7 years, GPHS modules experience less than 5% decrease in thermal energy over a ten year period, making $^{238}PuO_2$ fuel suitable for long duration space missions (5–15 years). Besides being heavy (as fabricated density of ~9700 kg/m^3 and thermal power density of ~0.4 kW_{th}/kg), domestic pro-

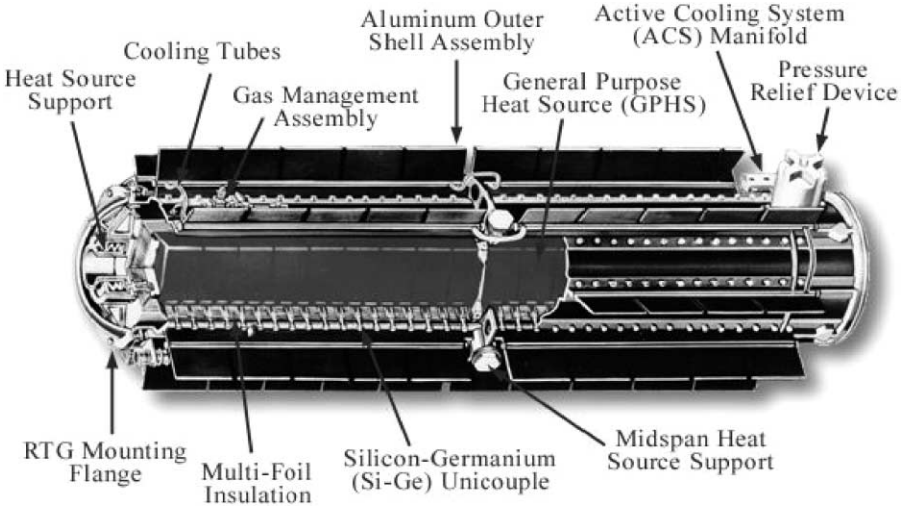

Fig. 1. Current RTGs with 18 GPHS modules and SiGe thermoelectric unicouples for generating 280 W_e at beginning of life (~5.5 W_e/kg).

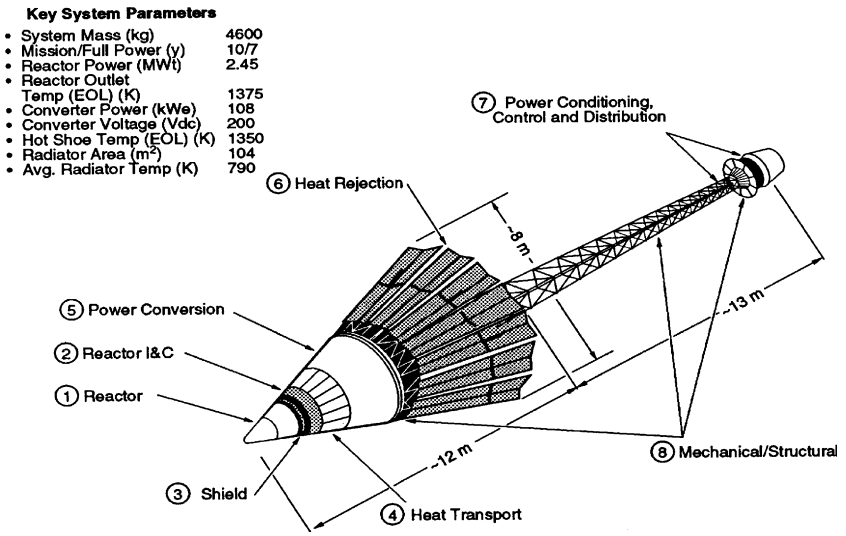

Fig. 2. SP-100 nuclear reactor power system developed in the United States in late eighties and early nineties with SiGe/GaP thermoelectric modules for an overall system efficiency of ~4.4% and specific power of ~23.5 W_e/kg.

duction of $^{238}PuO_2$ in the US has been halted for more than ten years and the cost of purchasing it from an external source has been quite high. In addition, since SiGe unicouples in RTGs (Fig. 1) operate at a conversion efficiency of <7%, a relatively large number of GPHS modules are required to meet certain electrical power requirements. For a typical requirement of 280 W_e, for example, more than 10 kg of $^{238}PuO_2$ in 18 GPHS modules would be needed [10,15] (Fig. 1).

Therefore, there is an interest to develop thermoelectric devices that are more efficient than SiGe unicouples for advanced RTGs. Higher conversion efficiency will reduce not only the number of GPHS modules needed for meeting certain electrical power requirements but also the heat rejection radiator size, thus decreasing the total mass and increasing the power density to >8 W_e/kg, which is >45% higher than that of present RTGs (~5.5 W_e/kg).

The performance of thermoelectric devices depends on the value of the hot side temperature, the temperature difference between the hot and cold ends, and the figure-of-merit, *ZT*, of the thermoelectric material used. Materials with higher *ZT* will give higher conversion efficiency and higher electrical power density. However, no single thermoelectric material has high *ZT* over a wide range of temperatures, each material typically possesses high *ZT* within a certain temperature range (Fig. 3). Therefore, segmented thermoelectric unicouples (STUs), in which the n- and p-legs are comprised of segments of various materials, could operate at higher conversion efficiency than a single material in the n- and p-legs. The number of the segments in the n- and p-legs, however, will depend on the values of the hot and cold side temperatures and the *ZT* of candidate thermoelectric materials.

Recently, skutterudite alloys have been developed at the Jet Propulsion Laboratory (JPL) in Pasadena, California, which have *ZT*s ranging from ~0.92 to 1.48 in the temperature range from 300 to 973 K [3,4,9,12] (see Fig. 3). In addition, a number of STUs have been fabricated using p-type $CeFe_4CoSb_{12}$ and Bi_2Te_3 based alloys and n-type $CoSb_3$ and Bi_2Te_3 based alloys. These STUs have been tested at cold and hot side temperatures of 300 and 973 K, respectively, demonstrating a conversion efficiency to date of ~10% [5–7]. Additional new thermoelectric materials with *ZT* values higher than for SiGe and suitable for operation above 973 K up to 1273 K are being developed at JPL to form eventually the top segment of STUs for use in future RTGs [13] and space nuclear reactor power systems. The resulting STUs will consist of 2–4 segments each, in

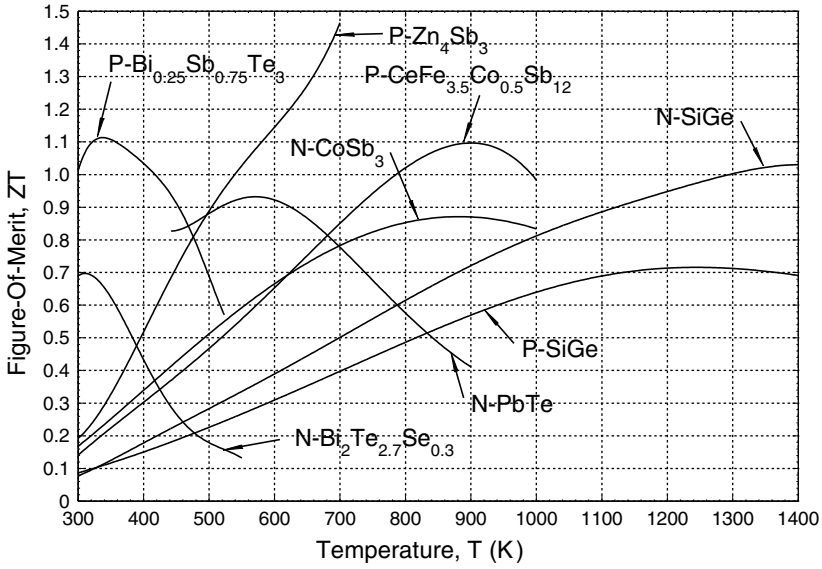

Fig. 3. Figure-of-merit of some thermometric materials.

the n- and p-legs, and operate between 1173–1273 and 573 K at a projected peak conversion efficiency >10%.

A one dimensional (1-D) analytical model and a 3-D finite element model of STUs have been developed, and the model predictions have been compared with some of the test data generated at JPL for STUs [8,14]. In addition, a global optimization methodology has been developed to calculate the lengths of the various segments in the n- and p-legs as well as the interfacial temperatures for maximum efficiency and maximum power density STU designs. This paper uses the 1-D model and the global optimization methodology to calculate the performance of the SiGe ($Si_{0.8}Ge_{0.2}$) unicouple [10,11] and compare it with that of STU, having the same total length and cross sectional area of the p-leg. The lengths of the various segments in the STUs and the cross sectional areas of the n-leg are determined for both maximum electrical power density and maximum conversion efficiency operations. The present comparisons assume zero side heat losses, which is the condition for fully integrated unicouples in RTGs, and a contact resistance of 150 $\mu\Omega\,cm^2$ per leg. The comparisons are performed at hot side temperatures, T_h, of 973 K and cold side temperatures, T_c, of 300, 573 and 673 K.

2. Results and discussion

Before conducting the performance comparison of the SiGe ($Si_{0.8}Ge_{0.2}$) unicouples and STUs, the 1-D model used herein [8] is benchmarked using the performance data reported for two SiGe unicouples [10,11]. These unicouples were tested for 3 and 1100 h, respectively, and the measurements included open circuit voltage, load voltage and electrical power at 2.469 and 2.483 A and the total resistance of the unicouple. Table 1 shows that for almost the same total unicouple resistance, the model predictions are in excellent agreement with the reported measurements, confirming the soundness of the model for conducting the present performance comparisons of SiGe (Fig. 4) and STUs (Figs. 5 and 8). The comparison results for maximizing the conversion

Table 1
Comparison of model predictions [8] with experimental data for two SiGe unicouples[a] in two separate tests

Performance parameters	3 h test (T_h = 1272.8 K and T_c = 573.6 K)		1100 h test (T_h = 1275.1 K and T_c = 569.5 K)	
	Experimental data [10]	Model predictions	Experimental data [10]	Model predictions
Open circuit voltage (V)	0.341	0.354	0.359	0.356
Current, I (A)	2.469	2.469	2.483	2.483
Load voltage, V_L (V)	0.202	0.217	0.203	0.202
Total resistance (Ω)	0.056	0.056	0.064	0.062
Electrical power (W_e)	0.500	0.535	0.503	0.502
Conversion efficiency (%)	–	7.65	–	7.13
Input power (W_{th})/flux (W_{th}/cm^2)	–	7.0/39.2	–	7.0/39.4
Rejected power (W_{th})/flux (W_{th}/cm^2)	–	6.5/36.2	–	6.5/36.6

[a] $A_p = A_n = 2.7432$ mm × 6.5024 mm, $L = 20.32$ mm [8].

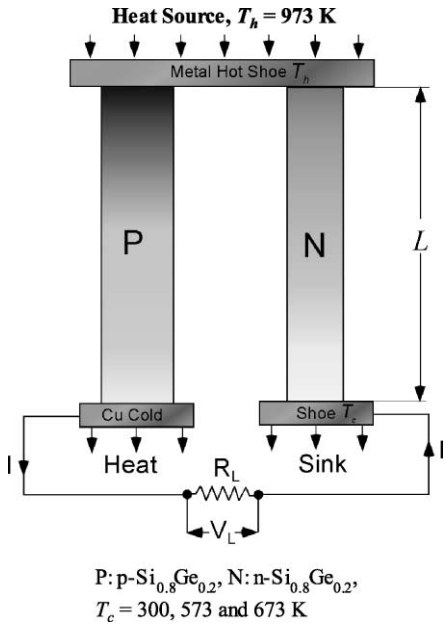

Fig. 4. A schematic of the SiGe unicouple.

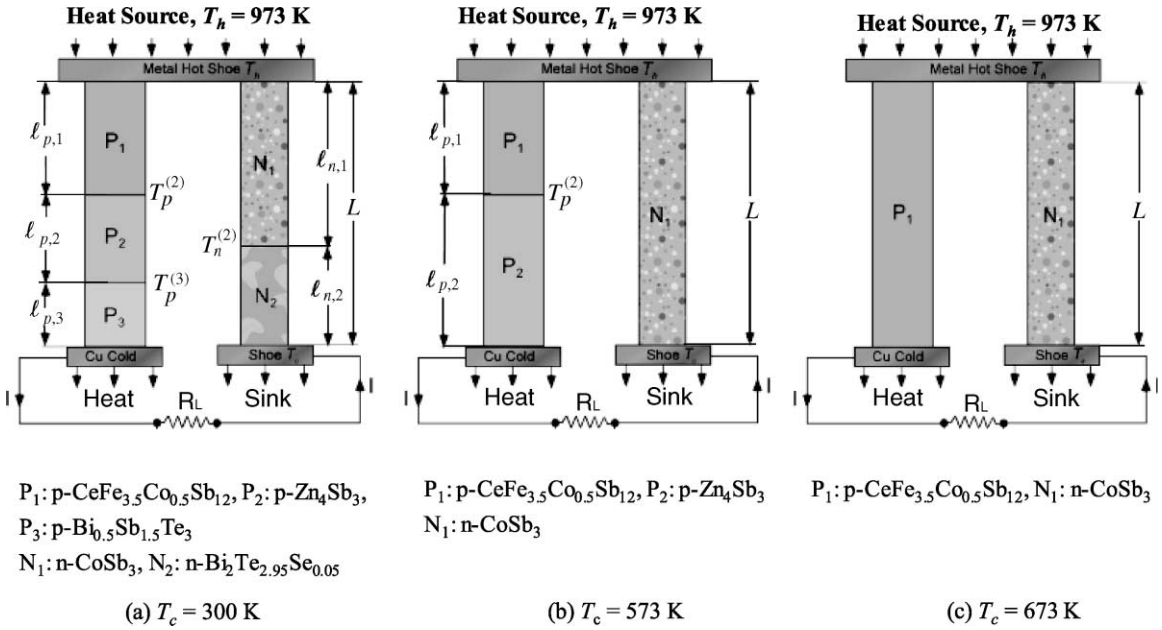

Fig. 5. A schematic of STUs for maximizing the conversion efficiency at $T_h = 973$ K.

efficiency are presented first in the next section, followed by those for maximizing the electrical power density.

2.1. Performance comparison for conversion efficiency maximization

The performance comparisons of SiGe unicouples and STUs are conducted at the same hot side and cold side temperatures, total length (20.32 mm), cross section area of the p-leg (2.74 mm × 6.5 mm) and total contact resistance of 150 $\mu\Omega\,cm^2$ per leg (Figs. 4 and 5). The base alloy of the SiGe unicouples is $Si_{0.8}Ge_{0.2}$, while the materials and the number of the various segments in the n- and p-legs of the STUs for maximizing the conversion efficiency varied with the cold side temperature in the analysis (Figs. 3 and 5). Fig. 4 shows a schematic of the SiGe unicouple, while Fig. 5a–c shows the STUs for maximized efficiency at cold side temperatures, $T_c = 300$, 573 and 673 K, respectively. These temperatures are typical of those that might be encountered by STUs in space probes, RTGs, and space nuclear reactor power systems, respectively. The hot side temperature of 973 K is the current limit of the skutterudite materials developed at JPL to date (Fig. 3), and their thermoelectric properties have been well characterized [3,4,9].

The calculated values of the conversion efficiency and the electrical power output of the SiGe unicouples (Fig. 4) and of the STUs (Fig. 5a–c) are delineated in Figs. 6 and 7. The results in these figures are based on maximizing the conversion efficiency of STUs, whose calculated dimensions and values of interfacial temperatures between segments in the n- and p-legs are listed in Table 2. In Figs. 6 and 7, the portions of the curves indicated by the solid and dashed lines represent the operation domains in which the unicouples are load following and non-load following, respectively. The solid circles mark the peak efficiencies, while the open triangles mark the peak electrical powers. The various performance parameters calculated at the peak conversion efficiency and the peak electrical power for the SiGe unicouple and STUs and shown in Figs. 4 and 5 are listed in Table 2.

Figs. 6 and 7 show that for the STUs, the peak electrical powers and those corresponding to the peak efficiencies are ~14% and 15% lower than those of SiGe (Fig. 7), when operating at $T_c = 300$ and 573 K, respectively. Conversely, the peak conversion efficiencies and those at the peak electrical powers of the STUs are almost twice and 55% higher than those of the SiGe unicouple (Fig. 6) at $T_c = 300$ and 573 K, respectively. When $T_c = 673$ K, the peak electrical powers of the SiGe unicouple and of the STU (Fig. 5c) are the same, but the peak conversion efficiency of the later is 40% higher than the former (Table 2). The results delineated in Figs. 5 and 6 indicate that increasing T_c from 300 to 573 K (typical for SiGe unicouples in current RTGs, Fig. 1) and to 673 K (typical for space nuclear reactor power systems, Fig. 2) decreases both the conversion efficiency and the electrical power output. Nonetheless, the performance of the STUs is superior to that of the SiGe unicouples (Table 2).

When $T_c = 300$ K, the peak conversion efficiency and that corresponding to the peak electrical power of the STU (Fig. 5a) are 14.69% and 14.44 %, respectively, versus 7.40% and 7.33% for the SiGe unicouple, respectively. Raising T_c to 573 and 673 K decreases the conversion efficiency of the STUs by ~47% and 63%, respectively, versus ~35% and 50%, respectively, for the SiGe unicouples. At these cold side temperatures, the calculated peak conversion efficiencies of the STUs and those at the peak electrical powers are ~7.78% and 7.62%, and 5.41% and 5.29%, respectively, while those for the SiGe unicouple are 5.03% and 4.98%, and 3.88% and 3.83%, respectively. Table 2 also indicates that the electrical power density of the STUs decreases from 97–99 to 22–22.6 W_e/kg, as T_c increases from 300 to 673 K, respectively, compared to 231–233 and 52.4–53 W_e/kg for the SiGe unicouple, respectively. Because the smear density of the STUs is

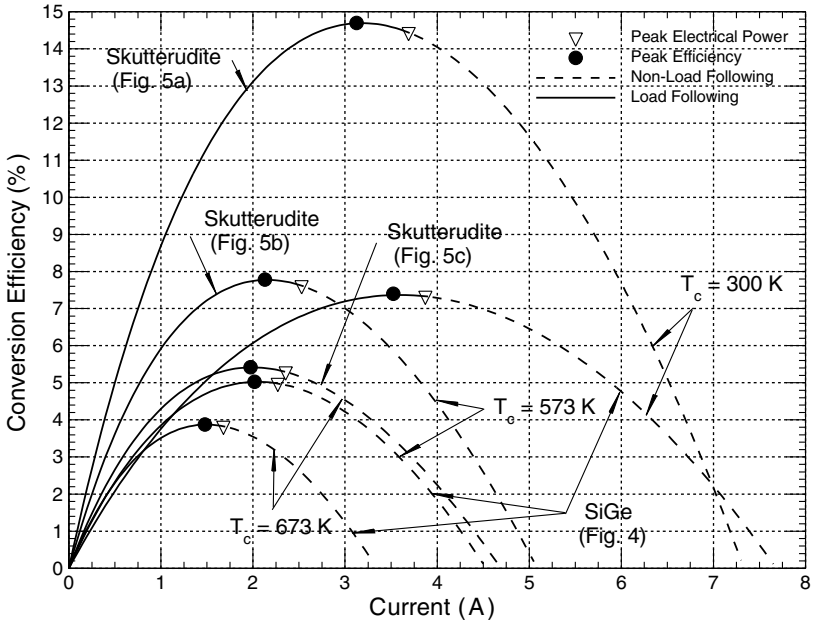

Fig. 6. Comparison of calculated conversion efficiency for SiGe and STUs operating at $T_h = 973$ K and designed for maximizing the conversion efficiency.

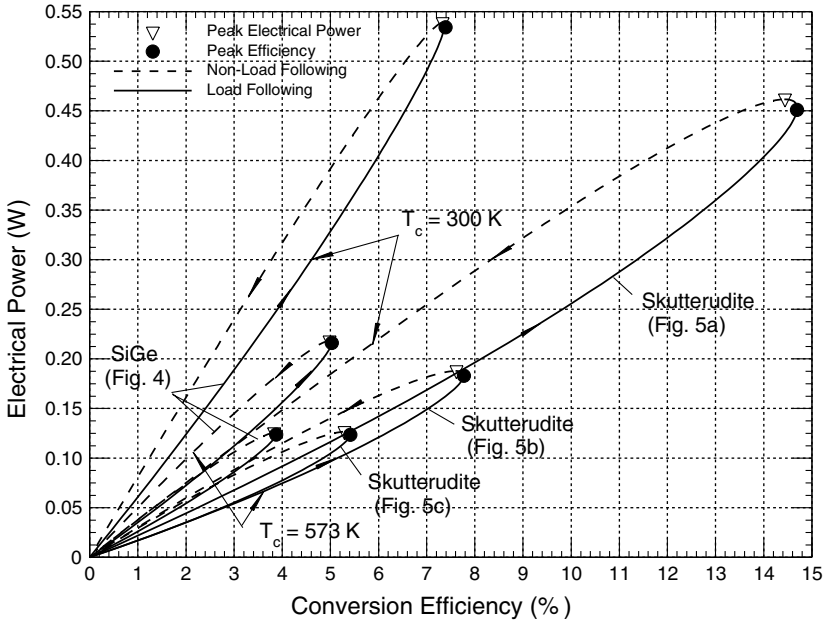

Fig. 7. Electrical power versus conversion efficiency for SiGe and STUs operating at $T_h = 973$ K and designed for maximizing the conversion efficiency.

Table 2
Performance comparison of STUs and SiGe unicouples designs for maximum efficiency optimization for $T_h = 973$ K and various T_c

Performance parameters	$T_c = 300$ K		$T_c = 573$ K		$T_c = 673$ K	
	STU (Fig. 5a)	SiGe (Fig. 4)	STU (Fig. 5b)	SiGe (Fig. 4)	STU (Fig. 5c)	SiGe (Fig. 4)
Power (W_e)						
At η_{peak} (*)	0.45 (0.85)	0.53 (1)	0.18 (0.85)	0.216 (1)	0.124 (1.00)	0.124 (1)
$(P_e)_{peak}$ (*)	0.46 (0.86)	0.54 (1)	0.19 (0.86)	0.218 (1)	0.127 (1.01)	0.126 (1)
Efficiency (%)						
η_{peak} (*)	14.69 (1.99)	7.40 (1)	7.78 (1.55)	5.03 (1)	5.41 (1.40)	3.88 (1)
At $(P_e)_{peak}$ (*)	14.44 (1.97)	7.33 (1)	7.62 (1.53)	4.98 (1)	5.29 (1.38)	3.83 (1)
Input heat flux (W_{th}/cm^2)						
At η_{peak} (*)	10.24 (0.537)	19.08 (1)	7.39 (0.669)	11.04 (1)	6.39 (0.778)	8.21 (1)
At $(P_e)_{peak}$ (*)	10.57 (0.547)	19.34 (1)	7.77 (0.691)	11.25 (1)	6.72 (0.796)	8.44 (1)
Input power (W_{th})						
At η_{peak} (*)	3.1 (0.423)	7.25 (1)	2.35 (0.549)	4.29 (1)	2.28 (0.714)	3.19 (1)
At $(P_e)_{peak}$ (*)	3.2 (0.435)	7.35 (1)	2.47 (0.565)	4.37 (1)	2.4 (0.731)	3.28 (1)
Rejected heat flux (W_{th}/cm^2)						
At η_{peak} (*)	8.66 (0.490)	17.68 (1)	6.82 (0.651)	10.48 (1)	6.05 (0.766)	7.90 (1)
At $(P_e)_{peak}$ (*)	9.05 (0.505)	17.92 (1)	7.17 (0.668)	10.73 (1)	6.36 (0.785)	8.10 (1)
Rejected power (W_{th})						
At η_{peak} (*)	2.62 (0.39)	6.72 (1)	2.17 (0.53)	4.07 (1)	2.16 (0.702)	3.07 (1)
At $(P_e)_{peak}$ (*)	2.74 (0.40)	6.81 (1)	2.28 (0.55)	4.17 (1)	2.27 (0.719)	3.15 (1)
Electrical power density (W_e/kg)/(W_e/cm^3)						
At η_{peak}	97/0.73	231/0.69	37/0.280	91.5/0.27	22.0/0.170	52.4/0.156
At $(P_e)_{peak}$	99/0.75	233/0.70	38/0.290	92.4/0.276	22.6/0.175	53.0/0.159
Dimensions						
A_p (mm^2)	17.837	17.837	17.837	17.837	17.837	17.837
A_n (mm^2)	12.426	20.167	13.972	21.015	17.856	21.032
$\ell_{p,1}$ (mm)	14.351	–	18.287	–	–	–
$\ell_{p,2}$ (mm)	2.720	–	2.033	–	–	–
$\ell_{p,3}$ (mm)	3.249	–	–	–	–	–
$\ell_{n,1}$ (mm)	19.281	–	–	–	–	–
$\ell_{n,2}$ (mm)	1.039	–	–	–	–	–
L (mm)	20.32	20.32	20.32	20.32	20.32	20.32
Interface temperatures (K)						
$T_p^{(2)}$	700	–	700	–	–	–
$T_p^{(3)}$	475	–	–	–	–	–
$T_n^{(2)}$	416	–	–	–	–	–
Temperature gradient (K/mm)						
$\Delta T_{p,1}/\ell_{p,1}$	19.0	33.1	14.9	19.7	14.8	14.8
$\Delta T_{p,2}/\ell_{p,2}$	82.7	–	62.5	–	–	–
$\Delta T_{p,3}/\ell_{p,3}$	53.9	–	–	–	–	–
$\Delta T_{n,1}/\ell_{n,1}$	28.9	33.1	19.7	19.7	14.8	14.8
$\Delta T_{n,2}/\ell_{n,2}$	111.6	–	–	–	–	–
Smear density (kg/m^3)	7577	2990	7693	2990	7735	2990

(*) Normalized to the value of the SiGe unicouple.

more than twice that of the SiGe unicouple, the power densities of the former in W_e/kg are lower than those for the latter. Conversely, when the power density is expressed in W_e/cm^3, the values for the STUs are only slightly higher than those for the SiGe unicouples at the same cold side temperatures (Table 2).

Table 2 also indicates that at $T_c = 300$ K, although the electrical power output of the SiGe unicouple is ~15% higher than that for the STU (Fig. 5a), the input and rejected thermal powers are ~130% and 156% higher, respectively. Therefore, despite the higher density of the STUs, their conversion efficiencies at $T_c = 300$ K are approximately twice those of the SiGe unicouples and both the input thermal power and the rejection thermal power are less than half those for the SiGe unicouple. At $T_c = 573$ K, the electrical power output of the SiGe unicouple is ~15% higher than that for the STU, but the conversion efficiency of the latter is ~54% higher than that of the former. In addition, the input and rejected thermal powers of the SiGe unicouple are ~82% and 87% higher than those for the STU (Fig. 5b). When $T_c = 673$ K, the electrical power output of the SiGe unicouple and the STU (Fig. 5c) are almost the same, but the conversion efficiency of the latter is ~39% higher, and the thermal and rejected powers are ~30% lower.

In summary, using skutterudite STUs instead of SiGe unicouples, in future space probes (Fig. 5a), in RTGs (Fig. 5b) and in space nuclear reactor power systems (Fig. 5c), could increase the conversion efficiency by ~55% when operating at $T_h = 973$ K and $T_c = 573$ K and by ~99% for $T_c = 300$ K. Thus, for a given electrical power requirement, the STU in Fig. 5b could potentially halve the mass of the $^{238}PuO_2$ fuel (or the reactor's thermal power) and the radiator surface area and mass in an RTG. It is worth noting that a SiGe unicouple operating at hot and cold temperatures of 1273 and 573.6 K, respectively (Table 1), has a slightly lower peak efficiency than a STU (Fig. 5b) operating at same cold side temperature but 300 K lower hot side temperature (Table 2).

Further examination of Table 2 and Fig. 3 shows that for maximizing the conversion efficiency of the STUs, the calculated interfacial temperatures of the segments in the n- and p-legs are the same as those at the intersections of the *ZT* curves of the thermoelectric materials of the segments. As shown in Table 2, the interface temperatures in the p-leg in the STU in Fig. 5a of 700 and 475 K and of 416 K in the n-leg are identical to those in Fig. 3 at the intersections of the *ZT* curves of the materials of the respective segments. As detailed in the next section, this finding is not applicable to STUs designed for maximizing the electrical power density (Fig. 8 and Table 3).

2.2. Performance comparison for maximum power density

The performance parameters of STUs (Fig. 8) and the SiGe unicouple (Fig. 4) for maximizing the electrical power density are compared in Figs. 9 and 10 and in Table 3. The results in Table 3 indicate that the configurations of the STUs for maximizing the conversion efficiency (Fig. 5a and b) are not applicable when maximizing the electrical power density at cold side temperatures of 300 and 573 K, respectively. The compositions of the n- and p-legs in the STUs for maximum power density operation are different from those for maximum efficiency (Fig. 8a and b versus Fig. 5a and b, respectively). As shown in Table 3, when the configuration of the STU in Fig. 5a is optimized for maximum power density operation, the length of the middle segment in the p-leg is very small (0.139 mm). In addition, the attainable peak electric power density of 108 W_e/kg is

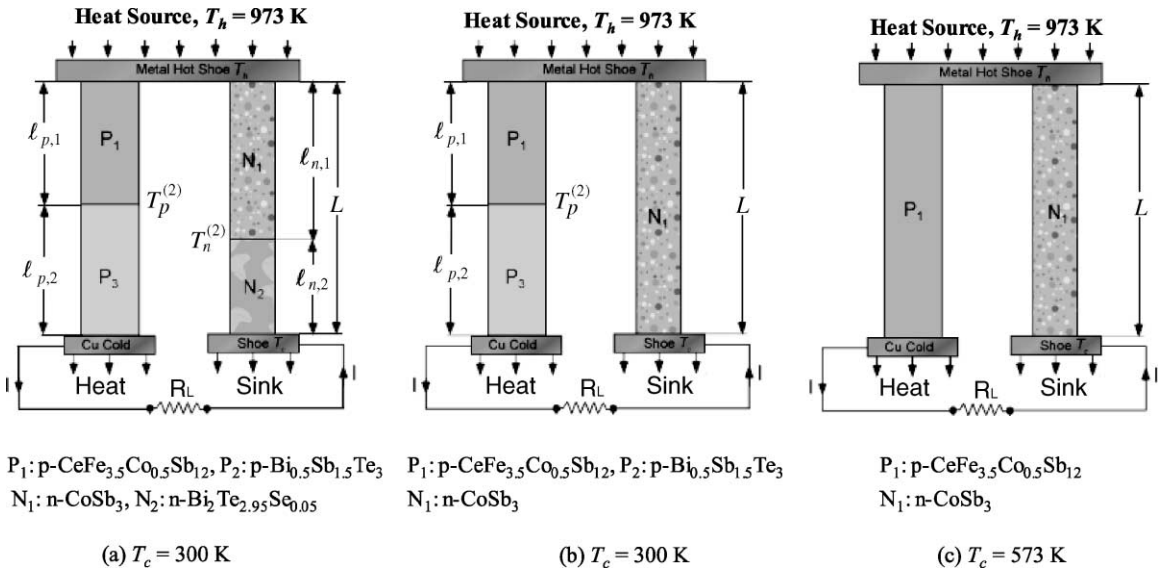

Fig. 8. A schematic of STUs for maximizing the electrical power density at $T_h = 973$ K.

slightly smaller than that for the configuration 8a (110 W_e/kg). The latter has only two segments in the p-leg, instead of the three segments in Fig. 5a, and the composition of the cooler segment in the p-leg in Fig. 8a is different than that in Fig. 5b. Furthermore, the interfacial temperatures in the n- and p-legs of the STU for maximized electrical power density (Figs. 5a or 8a and Table 3) are 50–198 K lower than those for maximized conversion efficiency (Table 2). As indicated earlier, the interfacial temperatures in the STU for maximizing the conversion efficiency are the same as those at the intersections of the *ZT* curves of the thermoelectric materials of the segments (Fig. 3).

In summary, the STU configurations for maximizing the electrical power density are relatively simpler than those for maximizing the conversion efficiency, and the interfacial temperatures of the segments in the n- and p-legs are much lower, increasing the temperature gradient in the segments (Tables 2 and 3). Therefore, STUs developed for maximum electrical power density operation are expected to experience higher thermal stresses than those designed for maximum efficiency operation, which will be the subject of a future contribution.

The results in Tables 2 and 3 show that the peak conversion efficiency of the STU operating at $T_c = 300$ K and optimized for maximum electric power density operation (Fig. 8a) of 13.68% is a percentage point lower than that for the STU configuration (Fig. 5a) for maximizing the efficiency operation (14.69%). On the other hand, the peak electrical power and power density for the former (0.66 W_e and 110 W_e/kg, respectively) are higher than those for the latter (0.46 W_e and 99 W_e/kg, respectively).

The results in Figs. 9 and 10 and Table 3 indicate that both the conversion efficiencies and electrical powers of the STUs are higher than those for the SiGe unicouple for all values of T_c investigated. For example, the peak electrical powers for the STU configurations (Fig. 10) in Fig. 8a (0.66 W_e) and 8c (0.24 W_e) are ~25% and 14% higher than that for the optimized SiGe (Fig. 4). In addition, the peak conversion efficiencies of the STUs (Fig. 9) in Fig. 8a and c of 13.13% and

Table 3
Performance comparison of STUs and SiGe unicouples designs for maximum electrical power density optimization for $T_h = 973$ K and various T_c

Performance parameters	$T_c = 300$ K				$T_c = 573$ K			$T_c = 673$ K	
	STU (Fig. 5a)	STU (Fig. 8a)	STU (Fig. 8b)	SiGe (Fig. 4)	STU (Fig. 5b)	STU (Fig. 8c)	SiGe (Fig. 4)	STU (Fig. 5c)	SiGe (Fig. 4)
Power (W_e)									
At η_{peak} (*)	0.63 (1.21)	0.65 (1.24)	0.62 (1.20)	0.52 (1)	0.23 (1.10)	0.24 (1.13)	0.22 (1)	0.13 (1.11)	0.12 (1)
$(P_e)_{peak}$ (*)	0.64 (1.22)	0.66 (1.25)	0.63 (1.21)	0.53 (1)	0.23 (1.11)	0.24 (1.14)	0.21 (1)	0.14 (1.12)	0.12 (1)
Efficiency (%)									
η_{peak} (*)	13.68 (1.86)	13.13 (1.78)	12.80 (1.74)	7.36 (1)	7.33 (1.46)	7.24 (1.44)	5.02 (1)	5.40 (1.40)	3.87 (1)
At $(P_e)_{peak}$ (*)	13.46 (1.84)	12.93 (1.76)	12.62 (1.72)	7.33 (1)	7.18 (1.44)	7.10 (1.43)	4.97 (1)	5.28 (1.38)	3.83 (1)
Input heat flux (W_{th}/cm^2)									
At η_{peak} (*)	12.09 (0.63)	12.91 (0.67)	13.13 (0.69)	19.13 (1)	8.37 (0.75)	8.51 (0.77)	11.10 (1)	6.47 (0.78)	8.25 (1)
At $(P_e)_{peak}$ (*)	12.51 (0.65)	13.33 (0.69)	13.53 (0.70)	19.39 (1)	8.72 (0.77)	8.86 (0.78)	11.31 (1)	6.75 (0.80)	8.45 (1)
Input power (W_{th})									
At η_{peak} (*)	4.61 (0.65)	4.92 (0.70)	4.88 (0.69)	7.07 (1)	3.13 (0.75)	3.26 (0.78)	4.17 (1)	2.47 (0.80)	3.10 (1)
At $(P_e)_{peak}$ (*)	4.77 (0.67)	5.08 (0.71)	5.03 (0.70)	7.17 (1)	3.26 (0.77)	3.40 (0.80)	4.25 (1)	2.58 (0.81)	3.18 (1)
Rejected heat flux (W_{th}/cm^2)									
At η_{peak} (*)	10.44 (0.59)	11.22 (0.63)	11.45 (0.65)	17.72 (1)	7.76 (0.74)	7.89 (0.75)	10.54 (1)	6.12 (0.772)	7.93 (1)
At $(P_e)_{peak}$ (*)	10.82 (0.60)	11.61 (0.65)	11.82 (0.66)	17.97 (1)	8.10 (0.75)	8.23 (0.77)	10.75 (1)	6.40 (0.788)	8.12 (1)
Rejected power (W_{th})									
At η_{peak} (*)	3.98 (0.61)	4.28 (0.65)	4.25 (0.65)	6.55 (1)	2.90 (0.73)	3.03 (0.76)	3.96 (1)	2.34 (0.79)	2.98 (1)
At $(P_e)_{peak}$ (*)	4.13 (0.62)	4.43 (0.67)	4.39 (0.66)	6.64 (1)	3.03 (0.75)	3.16 (0.78)	4.04 (1)	2.45 (0.80)	3.05 (1)
Power density (W_e/kg)/(W_e/cm^3)									
At η_{peak}	106/0.81	109/0.83	107/0.83	232/0.69	39/0.30	39/0.30	92/0.27	22.2/0.17	52.6/0.16
At $(P_e)_{peak}$	108/0.83	110/0.85	109/0.84	234/0.70	40/0.31	40/0.31	93/0.28	22.7/0.18	53.2/0.16
Dimensions									
A_p (mm^2)	17.837	17.837	17.837	17.837	17.837	17.837	17.837	17.837	17.837
A_n (mm^2)	20.309	20.291	19.328	19.135	19.564	20.513	19.724	20.429	19.759
$\ell_{p,1}$ (mm)	17.788	18.109	18.134	20.32	20.067	20.32	20.32	20.32	20.32
$\ell_{p,2}$ (mm)	0.139	–	–	–	0.253	–	–	–	–
$\ell_{p,3}$ (mm)	2.393	2.211	2.186	–	–	–	–	–	–
$\ell_{n,1}$ (mm)	19.808	20.036	20.32	20.32	20.32	20.32	20.32	20.32	20.32
$\ell_{n,2}$ (mm)	0.512	0.284	–	–	–	–	–	–	–
L (mm)	20.32	20.32	20.32	20.32	20.32	20.32	20.32	20.32	20.32
Interface temperature (K)									
$T_p^{(2)}$	502.5	478.0	475.8	–	594.5	–	–	–	–
$T_p^{(3)}$	484.4	–	–	–	–	–	–	–	–
$T_n^{(2)}$	366.3	339.9	–	–	–	–	–	–	–
Temperature gradient (K/mm)									
$\Delta T_{p,1}/\ell_{p,1}$	26.5	27.3	27.4	33.1	18.9	19.7	19.7	14.8	14.8
$\Delta T_{p,2}/\ell_{p,2}$	130.2	80.5	80.4	–	85.0	–	–	–	–
$\Delta T_{p,3}/\ell_{p,3}$	77.1	–	–	–	–	–	–	–	–
$\Delta T_{n,1}/\ell_{n,1}$	30.6	31.6	33.1	33.1	19.7	19.7	19.7	14.8	14.8
$\Delta T_{n,2}/\ell_{n,2}$	129.5	140.5	–	–	–	–	–	–	–
Smear density (kg/m^3)	7670	7682	7689	2990	7728	7732	2990	7732	2990

(*) Normalized to the value of the SiGe unicouple.

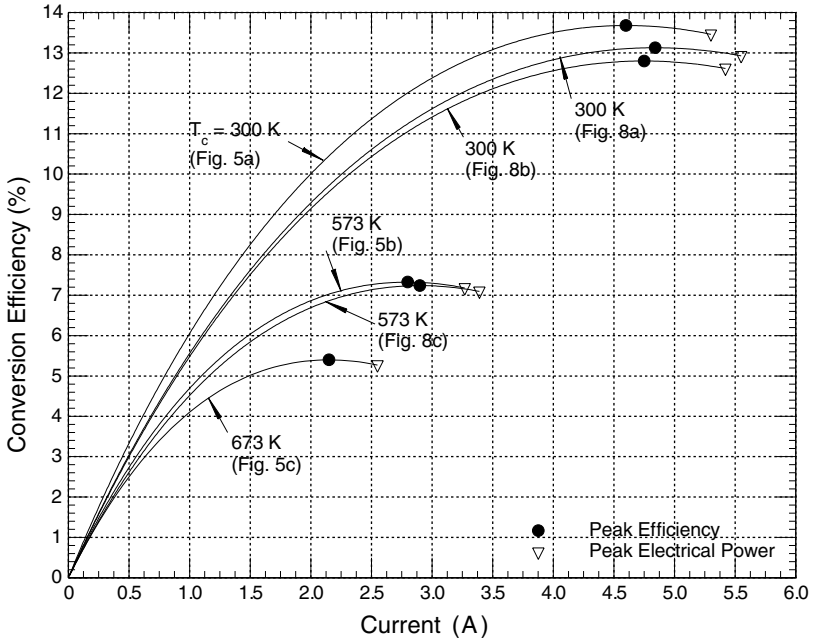

Fig. 9. The load following characteristics of STUs operating at $T_h = 973$ K and designed for maximizing the electrical power density.

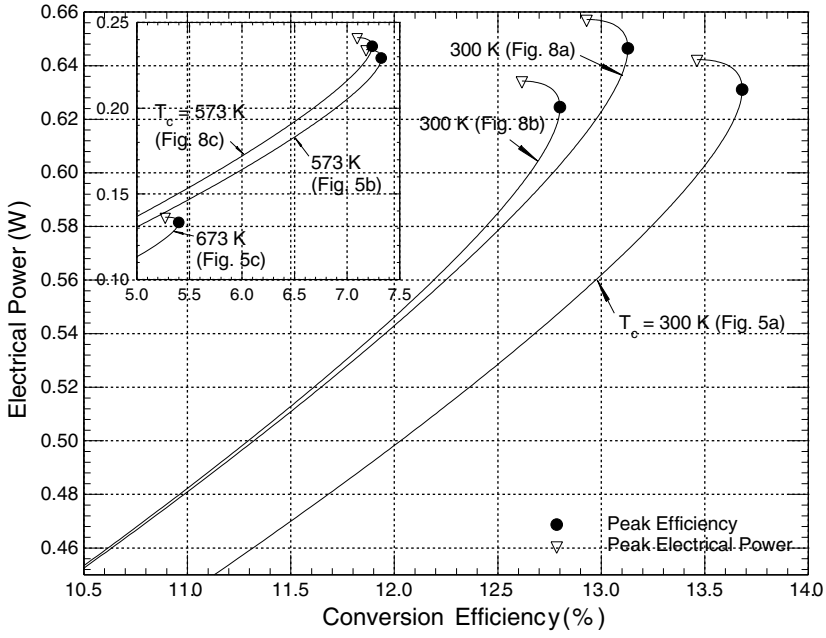

Fig. 10. Electrical power versus conversion efficiency for STUs operating at $T_h = 973$ K and designed for maximizing the electrical power density.

7.24% are ~78% and 44% higher, respectively, than that for the SiGe unicouple at the same cold side temperatures. Table 3 indicates that the peak electrical power densities of the STUs decrease from 110 to 40 and 22.7 W_e/kg as the cold side temperature increases from 300 to 573 and 673 K, respectively. These electrical power densities are lower, however, than those for the SiGe unicouples (234, 93 and 53.3 W_e/kg, respectively) at the same values of T_c (Table 3). Conversely, the peak electrical powers of the STUs at $T_c = 300$, 573 and 673 K of 0.66, 0.24 and 0.136 W_e are ~25%, 14% and 11.5%, respectively, higher than those for the SiGe unicouple (Table 3 and Fig. 10). Figs. 6 and 9 show that increasing the cold side temperature decreases the peak conversion efficiencies and peak electrical powers and shifts them to lower electrical current.

2.3. Load following

The portions of the performance curves shown in solid lines in Figs. 6, 7, 9 and 10 extending to the peak electric power, indicate the operation region where the unicouples are load following. In this region, as the load demand (or electrical current) increases, the electric power delivered by the unicouple increases. The conversion efficiency also increases with increased load demand up to the peak efficiency, but the efficiency decreases slightly as the load demand increases further to the peak electrical power. Beyond the peak electrical power, the unicouples are non-load following because the electrical power delivered decreases as the electrical current (or the load demand) increases. This region is marked in Figs. 6 and 7 by the dashed portions of the performance curves. The peak electrical power occurs when the effective load resistance equals the total internal resistance of the unicouple. Below the peak electrical power, or in the load following region, the load resistance is higher than the internal resistance of the unicouple. Hence, reducing the load resistance, as a result of connecting additional users in parallel, increases the electrical current, which, in turn, increases the electrical losses and joule heating in the unicouple but, at the same time, increases the electrical power output, both of which are proportional to the square of the current. At the peak efficiency, the increase in electrical power output as a result of reducing the load resistance (or increasing the load demand) balances the electrical losses in the unicouples. A further increase in the load demand, or decrease in the load resistance, increases the losses in the unicouple more than the electrical power output. Therefore, for energy conversion applications, the nominal operation point should be selected below the peak conversion efficiency, allowing the converter to operate in the load following region when the demand exceeds the nominal value, at the expense of only a small decrease in the conversion efficiency.

For example, if the STU in Fig. 5a operates nominally at the peak efficiency of 14.69%, the corresponding electrical power is 0.45 W_e. When the load demand increases to the peak electrical power of 0.46 W_e, which is equivalent to an increase of only 2.2% of the nominal, the conversion efficiency decrease by ~1.7% to 14.44%. However, to allow for a typical 10% increase in nominal electrical power in the load following region, the nominal operation point should be selected at an efficiency of 13%, where the electrical power of the STU is 0.362 W_e (Fig. 7). Similarly, for the STU in Fig. 8a, to allow for a 10% increase in the nominal electrical power in the load following region, the nominal operation point should be selected at a conversion efficiency of 12.65%, where the electric power for the unicouple of 0.594 W_e is 90% of the peak electrical power of 0.66 W_e (Table 3 and Fig. 10).

2.4. Performance domain

The results presented in Fig. 11 provide two surfaces for the operation domain of the STUs, one for the maximized efficiency designs and the other for the maximized electrical power density designs. These domains are bound on the left by solid lines, indicating the values for the maximized efficiency designs, and on the right by dashed lines, indicating the efficiencies for the maximized power density designs. These performance domains are enclosed at the top with the lines for $T_c = 300$ K and at the bottom by those for $T_c = 673$ K. At this cold side temperature, the performance lines for the maximized efficiencies and electrical power densities actually overlap, while at 300 K, the maximized efficiency lines are shifted to the left toward lower electrical power but higher conversion efficiency.

Fig. 11 indicates that as the cold side temperature decreases, both the electrical powers and conversion efficiencies for either maximizing the efficiency or the electrical power density increase. In addition, the difference between the peak conversion efficiencies and those at the peak electrical powers increases as the cold side temperature decreases.

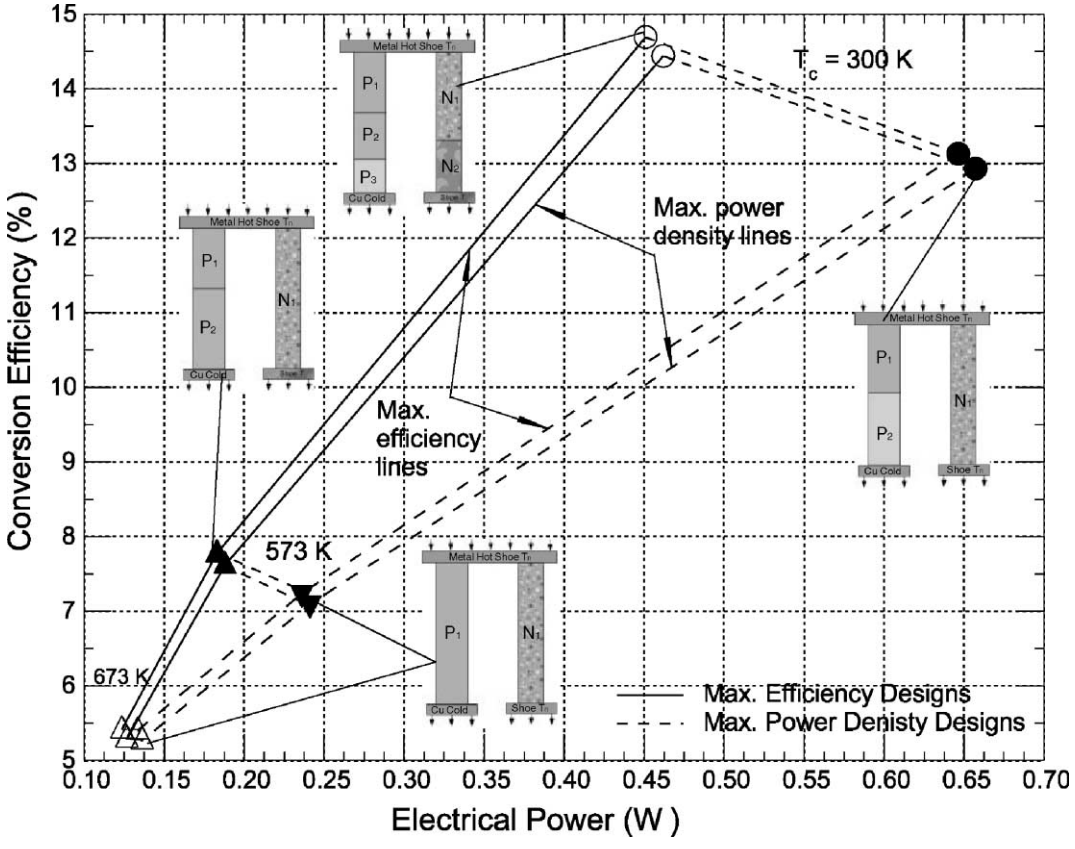

Fig. 11. Performance domain of STUs operating at $T_h = 973$ K and designed for maximizing both the conversion efficiency and the electrical power density.

3. Summary and conclusions

The performance parameters of a SiGe ($Si_{0.8}Ge_{0.2}$) unicouple and skutterudite STUs, operating at hot side temperature of 973 K and cold side temperatures of 300, 573 and 673 K are calculated and compared. These unicouples have the same total length and cross sectional area of the p-leg. The cross sectional area of the n-leg and the lengths of the various segments in the n- and p-legs in the STUs are optimized for both maximizing the efficiency and the electrical power density. The present comparisons assume zero side heat losses and a total contact resistance per leg of 150 $\mu\Omega\,cm^2$.

The present analyses are conducted using a 1-D analytical model and a global optimization methodology of the STUs that for given hot and cold side temperatures, total length and the thermoelectric materials in the various segments, determines the lengths of the segments and calculates the interfacial temperatures. Before conducting the performance comparison of the SiGe ($Si_{0.8}Ge_{0.2}$) unicouple and the STUs, the predictions of the analytical model are successfully benchmarked using reported performance data for two SiGe unicouples similar to those used in current RTGs and tested for 3 and 1100 h, respectively. The model predictions of the electrical power output, open circuit voltage and the load voltages at 2.469 and 2.483 A are in excellent agreement with the reported measurements.

The results indicate that the number of segments in the n- and p-legs of the STUs decreases as the cold side temperature increases. When the STUs are optimized for maximizing the conversion efficiency, the interfacial temperatures of the segments are the same as those at the intersections of the *ZT* curves of the materials of the segments. When optimized for maximizing the electrical power density, the number and the composition of some of the segments are different and the interfacial temperatures between segments in the n- and p-legs of the STUs are 50–198 K lower than for the STUs optimized for maximizing the conversion efficiency. The number of segments in the n- and p-legs of the latter are more than that for the former. Therefore, the configurations of STUs designed for maximizing the conversion efficiency are different from those for maximizing the electrical power density at the same cold and hot side temperatures.

For maximized efficiency designs at $T_c = 300$ K, although the electrical power output of the SiGe unicouple is ~15% higher than that for the STU, the input and rejected thermal powers are as much as 130% and 156% higher, respectively. Therefore, despite the higher density of the STUs, their conversion efficiencies at $T_c = 300$ K are approximately twice those of the SiGe unicouple and both the input and rejected thermal powers are less than half those for the SiGe unicouple. At $T_c = 573$ K, typical of that in current RTGs, the electrical power output of the SiGe unicouple is ~15% higher than that for the STU, but the conversion efficiency is ~46% lower. In addition, the input and rejected thermal powers for the SiGe unicouple are ~82% and 87% higher than those for the STU. When $T_c = 673$ K, the electrical power output of SiGe unicouple and STU are almost the same, but the conversion efficiency of the latter is ~39% higher, and the thermal and rejected powers are ~30% lower.

The peak conversion efficiency and that corresponding to the peak electrical power of the STUs at $T_c = 300$ K are 14.69% and 14.44 %, respectively, versus 7.40% and 7.33% for the SiGe unicouple, respectively. Raising T_c to 573 and 673 K decreases the conversion efficiency of the STUs by ~47% and 63%, respectively, and by ~32% and 47%, respectively, for the SiGe unicouple. The electrical power density of the STUs decreases from 97–99 to 22–22.6 W_e/kg as T_c increases from

300 to 673 K, respectively, compared to 231–233 and 52.4–53 W_e/kg for the SiGe unicouple, respectively. Because the smear density of the STUs is more than twice that of the SiGe unicouple, the power densities of the former in W_e/kg are lower than those for the latter. Conversely, when the power density is expressed in W_e/cm^3, the values for the STUs are only slightly higher than those for the SiGe unicouple, at the same cold side temperatures.

The results suggest that for a hot side temperature of 973 K, using STUs instead of SiGe unicouples in future space probes ($T_c < 300$ K), radioisotope power systems ($T_c \sim 573$ K) and space nuclear reactor power systems ($T_c \sim 673$ K) could increase the conversion efficiency by >99%, 55% and 41%, respectively. Thus, for a given electrical power, STUs could potentially more than halve the mass of the $^{238}PuO_2$ fuel (or the reactor's thermal power) and the surface area for the heat rejection radiator. The lower nuclear reactor thermal power decreases the fuel burnup in the reactor, thus increasing the useful lifetime of the space power system and/or decreasing the fuel mass.

Acknowledgements

This research is funded by the NASA Cross-Enterprise Development Program under grant no. NAG3-2543 to the University of New Mexico's Institute for Space and Nuclear Power Studies. A portion of the work performed at the Jet Propulsion Laboratory, California Institute of Technology, was sponsored by DARPA through an agreement with the National Aeronautics and Space Administration.

References

[1] Angelo JA, Buden D. Space nuclear power. Malabar, FL: Orbit Book Company, Inc; 1985. p. 159–97 (Chapter 9).
[2] Bennett T. Space applications. In: Rowe DM, editor. CRC Handbook of Thermoelectrics. Boca Raton: CRC Press; 1994. p. 515–37.
[3] Caillat T, Fleurial J-P, Borshchevsky A. Preparation and thermoelectric properties of semiconducting Zn_4Sb_3. J Phys Chem Solids 1997;58:1119–25.
[4] Caillat T, Fleurial J-P, Snyder J, Zoltan A, Zoltan D, Borshchevsky A. Development of a high efficiency thermoelectric unicouples for power generation applications. In: Ehrlich A, editor. Proceedings 18th International Conference on Thermoelectrics. Piscataway: IEEE; 1999. p. 473–6.
[5] Caillat T, Borshchevsky A, Snyder J, Fleurial J-P. High efficiency segmented thermoelectric unicouples. In: El-Genk MS, editor. Proceedings Space Technology and Applications International Forum (STAIF-2000), AIP Conference Proceedings No 504. New York: American Institute of Physics; 2000. p. 1508–12.
[6] Caillat T, Borshchevsky A, Snyder J, Fleurial J-P. High efficiency segmented thermoelectric unicouples. In: El-Genk MS, editor. Proceedings Space Technology and Applications International Forum (STAIF-2001), AIP Conference Proceedings No 552. New York: American Institute of Physics; 2001. p. 1107–12.
[7] Caillat T, Borshchevsky A, Snyder J, Fleurial J-P. Development of high efficiency segmented thermoelectric unicouples. In: Proceedings 20th International Thermoelectric Conference. Beijing, China: IEEE; 2002, in press.
[8] El-Genk MS, Saber HH. Performance optimization of segmented thermoelectric unicouples. In: El-Genk MS, editor. Proceedings Space Technology and Applications International Forum (STAIF-2002), AIP Conference Proceedings. New York: American Institute of Physics; 2002. p. 980–8.
[9] Fleurial J-P, Borshchevsky A, Caillat T, Ewell R. New materials and devices for thermoelectric applications. In: Proceedings 32nd Intersociety Energy Conversion Engineering Conference. New York: American Institute of Chemical Engineers; 1997. p. 1080–5.

[10] General purpose heat source radioisotope thermoelectric generator (GPHS-RTG) final design review. General Electric Company, Space Systems Division, Advanced Energy Program Department, Valley Forge, PA, 28–30 October 1980.
[11] Kelly CE. The MHW converter (RTG). In: Proceedings of 10th Intersociety Energy Conversion Engineering Conference. New York: American Institute of Chemical Engineers; 1975. p. 880–6.
[12] Smith GE, Wolfe R. Thermoelectric properties of bismuth–antimony alloys. J Appl Phys 1962;33:841–4.
[13] Shield V. Personal Communications. The Jet Propulsion laboratory, California Institute of Technology, Pasadena, CA, 2000.
[14] Saber HH, El-Genk MS. A three-dimensional, performance model of segmented thermoelectric converters. In: El-Genk MS, editor. Proceedings Space Technology and Applications International Forum (STAIF-2002), AIP Conference Proceedings. New York: American Institute of Physics; 2002. p. 998–1006.
[15] Schock A. Design evolution and verification of the general purpose heat source. In: Proceedings 15th Intersociety Energy Conversion Engineering Conference. American Institute of Aeronautics and Astronautics; 1980. p. 1508–12.